

An Investigation of the Mechanism Magnetite Precipitation Using Ammonium Carbonate

L.A. Frolova*, A.V. Derimova, T.E. Butyrina, M.O. Savchenko

Ukrainian State University of Chemical Technology, 49005, Gagarin ave., 8, Dnepr, Ukraine

Article info

Received:
10 February 2018

Received in revised form:
15 April 2018

Accepted:
2 June 2018

Abstract

The purpose of this study is to determine the phase composition of iron oxide compounds formed during precipitation by ammonium carbonate hydrolysis products, to establish the magnetite formation regions and the kinetic characteristics of the reaction formation Fe_3O_4 . Characterization by X-ray diffraction (XRD) indicated that magnetite is formed in a solution of ferrous sulphate during the hydrolysis of ammonium carbonate. It has a homogeneous phase composition and a cubic crystal structure. Phase diagrams of the formation of the crystalline phase of magnetite, goethite and ferric hydroxide have been determined. It has been established that magnetite with a spinel structure is formed under controlled slow precipitation from ferrous sulphate with an ammonium carbonate solution. The calculation of the kinetic characteristics of the reactions of solid phase precipitation (a rate constant at different initial concentrations of ferrous sulphate, the order of the reaction) has shown that the process proceeds in two stages with the formation of an intermediate compound and its further oxidation. Moreover, the rate constant of oxidation is 0.654 L/min mol, and the rate constant of the first reaction is much higher – 1.645 L/min mol.

1. Introduction

Currently, the field of iron oxide pigments use is expanding. This is due primarily to the huge range of technological applications, which is determined both by the reducing and by oxidizing properties of iron oxygen compounds, by the variety of phase modifications (gamma, alpha, beta and sigma). Iron oxide pigments are available, versatile, resistant to external conditions, corrosion-resistant, have a wide range of colors from yellow, orange, red to violet, brown and black [1, 2]. In addition, a special group consists of iron oxide pigments that have magnetic properties (maghemite $\gamma\text{-Fe}_2\text{O}_3$, magnetite Fe_3O_4) [3–6]. Special properties are determined primarily by the dispersed and phase composition. The optimal conditions for obtaining the most demanded magnetite iron oxide pigments on the market are the subject of many studies [7–18].

The author's analysis of the results, studying the influence of various factors on the magnetite quality, suggests that the nature of the precipitator is very important in the technology of obtaining

magnetite [19–23]. The choice of an appropriate reagent is influenced by the following factors: a reaction rate, an ability to the buffer effect an ability to the buffer effect when maintaining a constant pH, the solubility, the price and availability of a reagent, easy and inexpensive transportation of a reagent. In practice, the production of iron oxide pigments use quicklime CaO , lime $\text{Ca}(\text{OH})_2$, soda ash Na_2CO_3 , caustic soda NaOH , ammonia NH_4OH , and calcined magnesite MgO .

All of the above reagents have both advantages and disadvantages. When using inexpensive precipitants, such as calcium hydroxide, calcium oxide, quenched dolomitic lime, or dolomitic lime, a poor quality pigment is formed contaminated with poorly soluble calcium and magnesium sulphates. The use of ammonia complicates the technological scheme and requires complex and expensive transportation of reagent. Homogeneous methods of precipitation of iron oxides and hydroxides are promising, for example, those using products of high-temperature hydrolysis of ammonium carbonate and urea. This allows us to regulate the process of seed formation and their further growth.

*Corresponding author. E-mail: 19kozak83@gmail.com

2. Experimental Methods

In the experimental studies, the following reagents were used: $\text{FeSO}_4 \cdot 7\text{H}_2\text{O}$ (reagent grade); Trilon B (analytical grade); ammonium carbonate (reagent grade), KMnO_4 (analytical grade), H_2SO_4 (analytical grade).

The following conditions were used in the studies: the concentration of FeSO_4 – 0.5 mol/L, the concentration of $(\text{NH}_4)_2\text{CO}_3$ – 4.0 mol/L, temperature – 15–100 °C. The molar ratio n was determined by the Eq. 1:

$$n = \frac{M_{(\text{NH}_4)_2\text{CO}_3}}{M_{\text{FeSO}_4}} \quad (1)$$

Air was used as the oxidizing agent, its effective feed rate in all the experiments was 10 L/min⁻¹. The mixture obtained was heated to a predetermined temperature which was maintained throughout the entire process. The compressor was then connected to oxidize the mixture with air. The oxidation time was 30–40 min. Reactions of precipitation were performed at different temperatures, time in a thermostatic cell equipped with temperature-compensated electrode systems to measure and record the pH and the redox potential of the system and with stirrer having rotation speed of 300 rev/min. The cell was provided with an input device and that of recording the amount of bubbling air [24]. After that, the mixture was filtered, the resulting paste was dried at 150 °C and then ground.

Kinetic studies were carried out by sampling at regular intervals. The determination of the ferrous sulphate concentration was carried out by the permanganatometric method [25]. The X-ray diffraction analysis was carried out using a DRON-2 diffractometer.

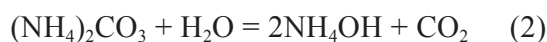
3. Results and discussion

The kinetic dependences of the total process, as well as the modeling of the experimental data obtained, make it possible to study the mechanism of the flow of homogeneous precipitation with ammonium carbonate, as well as the influence of various factors, determine the order and the constant of the process rate, the number and the nature of the intermediate products, the activation energy, determine the influence of the precipitant nature, as well as the nature and number of ongoing reactions.

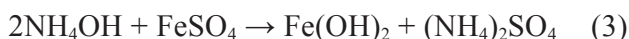
In many cases, the process of precipitation from solutions of ferrous salts with ammonium carbonate is simplified, suggesting that the reaction

produces ferrous carbonate. However, due to the ability of both the carbonate ion and ammonium to hydrolyze, there are not only carbonate ions, but also bicarbonate ions and hydroxyl ions present in the solution. This can lead to the formation of both ferrous carbonate and ferrous hydroxide, as well as basic iron carbonate. However, this is only true in the complete absence of oxygen in solution and at low temperatures. In the presence of oxygen, Fe^{2+} ions are oxidized in solution and suspension, which greatly complicates the whole system. Often, the resulting layered double hydroxides are the pre-structure of the resulting spinel structure.

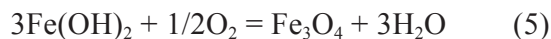
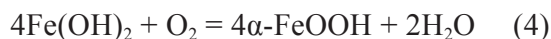
The general scheme for the precipitate formation from the solutions of ferrous salts with ammonium carbonate can be presented as follows. The reaction of hydrolysis of ammonium carbonate:



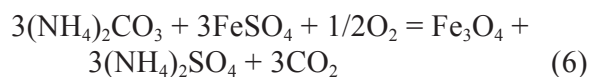
The second step is the formation of ferrous hydroxide or the basic ferrous salt, depending on the precipitant/ferrous sulfate mole ratio:



The third stage is the oxidation of the ferrous compounds to trivalent iron by one of several possible schemes:



The overall reaction of Fe_3O_4 formation:



Due to the possibility of formation, as a result of synthesis, of iron oxyhydroxides, ferrous hydroxides, ferric hydroxides, magnetite, and basic salts (II), it was necessary to establish the conditions for the formation of magnetite at the first stage of the studies (Fig. 1).

The conducted studies show that the phase composition of the product obtained depends to a large extent on the temperature of the solution, the molar ratio of the reacting components and the duration of the air supply. In the range of $t = 15\text{--}25$ °C and at $n = 2\text{--}5.5$ – a heterogeneous precipitate of $\text{Fe}(\text{OH})_2$ and $\text{Fe}(\text{CO}_3)_x(\text{OH})_{2-2x}$ is formed (bubble aeration time – 10–15 min); at $t = 60\text{--}90$ °C and at $n = 2\text{--}3.75$ – goethite ($\alpha\text{-FeOOH}$) is the product (20–30 min of bubble aeration); at a higher temperature and a greater molar ratio – magnetite Fe_3O_4 is formed. For $n < 2$, $\text{Fe}_2(\text{SO}_4)_3$ is formed.

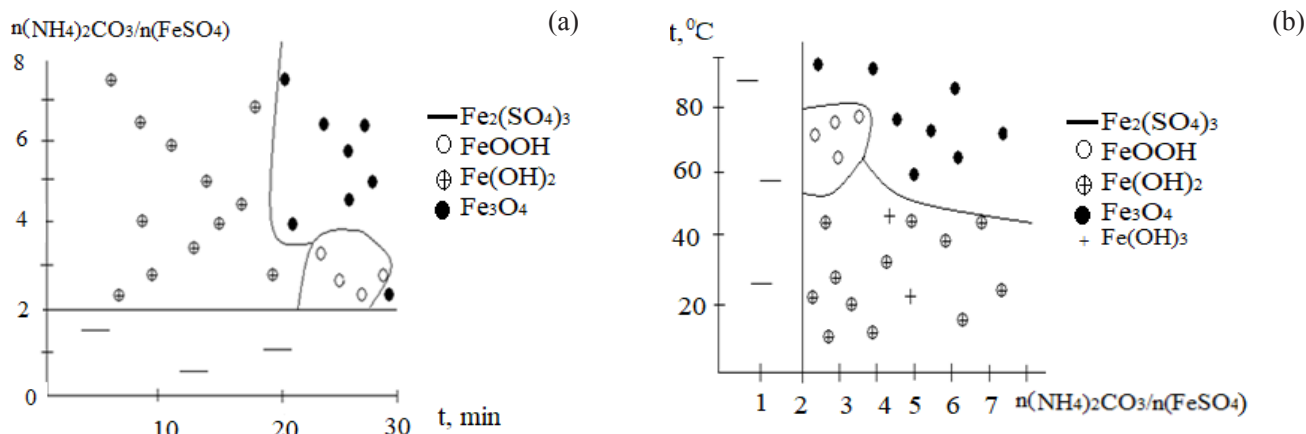


Fig. 1. Dependence of the phase composition of the resulting precipitate in the system $\text{FeSO}_4\text{-(NH}_4)_2\text{CO}_3\text{-H}_2\text{O-O}_2$ on the time of air supply and the ratio of components, $t = 80^\circ\text{C}$ (a), the temperature and the time of air supply (b), $\tau = 30$ min, duration of air – 10 min^{-1} .

In this way, the formation of magnetite passes through the whole range of the n values above stoichiometric ($n = 2\text{--}8$), the temperature values – $60\text{--}100^\circ\text{C}$, the processing time – 30 min. These conditions are adopted to simulate the kinetics of the process. The adopted technique is used to study homogeneous processes; therefore, this technique is used for homogeneous reactions, but it can also be used for heterogeneous processes if the limiting reaction is known. The ratio of the reacting components chosen under the conditions of the experiments equals 8.

The XRD analysis of the product showed the presence of magnetite phase. The slight broadening of the XRD lines (Fig. 2) can be interpreted in terms of poor crystallinity of the precipitated magnetite and small size of crystallites. The weak diffuse scattering at small angles indicates the presence of a small amount of matter in the X-ray amorphous state in the obtaining sample studied along with the crystalline phases.

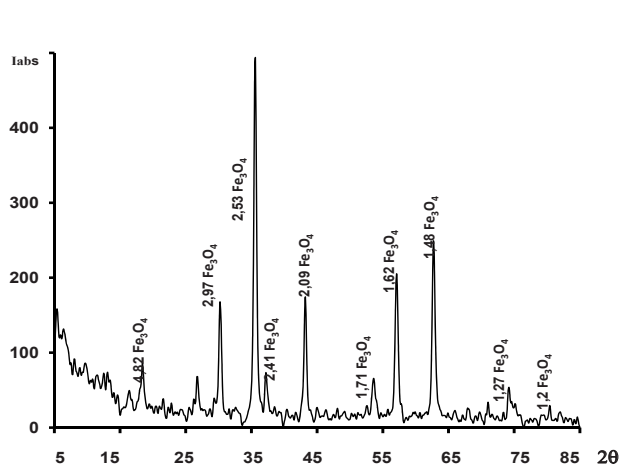


Fig. 2. X-ray pattern for samples magnetite ($\text{Cu-K}\alpha$ – radiation).

To determine the kinetic characteristics of the chemical reaction, dependence of the residual iron concentration on the duration of the process for different initial concentrations of ferrous sulfate at 100°C was obtained (Fig. 3).

Kinetic dependence of the residual concentration of ferrous cations characterizes the total process of converting the reacting substances to the final product of their interaction – black iron oxide pigment; irrespective of the initial concentrations, the kinetic curves have a similar character. However, the initial concentrations of ferrous sulphate significantly influence the yield of the desired product. It can be concluded that the greater the initial concentration of the reagent, the fuller the process of converting the reacting substances into the desired product, magnetite, proceeds. This conclusion is also confirmed by the fact that the yield of the product increases with increasing concentration of the starting substance and reaches 95% with the initial concentration of ferrous sulfate 0.45 mol/L (Fig. 3).

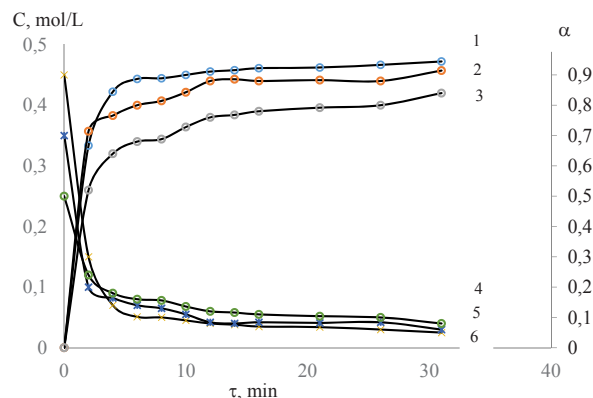


Fig. 3. Dependence of residual concentration of ferrous sulfate on time (1, 2, 3) and product yield (α) on time (4, 5, 6); 1 and 6 – 0.45 mol/L ; 2 and 5 – 0.35 mol/L ; 3 and 4 – 0.25 mol/L ; $t = 100^\circ\text{C}$; $n = 8$.

Table
Rate constants for reactions (R^2 is linear correlation coefficient)

Initial concentration, mol/L	LnC- τ		1/C- τ		1/C ² - τ	
	K	R ²	K, L/min mol	R ²	K, L/min mol	R ²
0.25	-0.0727	0.6562	1.3557	0.933	68.411	0.9772
0.35	-0.0645	0.7089	1.0449	0.9435	43.04	0.99
0.45	-0.0639	0.856	0.9912	0.9758	37.299	0.975

To understand the mechanism of the reactions taking place, it is necessary to determine the order of the limiting reaction and its rate constant. For this, was used the integration method. To determine the apparent order of the reaction and the reaction rate constant, the data were processed in the coordinates of $\ln C-\tau$, $1/C-\tau$, and $1/C^2-\tau$. However, in this case, it was not possible to satisfactorily describe the obtained data by any of the proposed dependencies (Figs. 4–6, Table). This can be explained by the complexity and multistage nature of the ongoing processes (Eqs. 2–6).

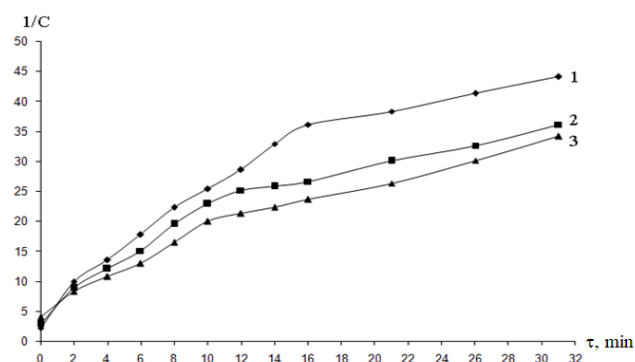


Fig. 4. Dependence of the inverse concentration of ferrous sulfate on the process time $t = 100\text{ }^\circ\text{C}$; $n = 8$; initial concentration of ferrous sulphate: 1 – 0.45 mol/L; 2 – 0.35 mol/L; 3 – 0.25 mol/L.

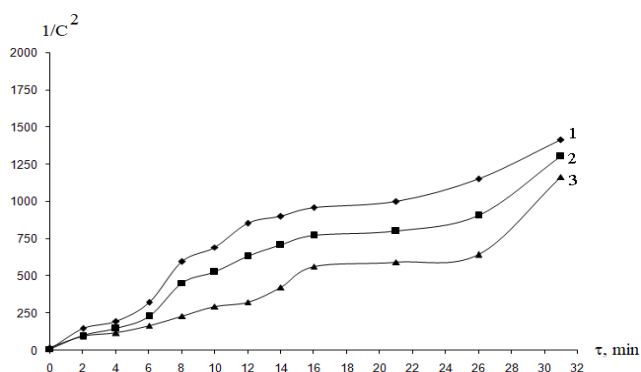


Fig. 5. Dependence of the square of the inverse concentration of ferrous sulfate on the process time $t = 100\text{ }^\circ\text{C}$; $n = 8$; initial concentration of ferrous sulphate: 1 – 0.45 mol/L; 2 – 0.35 mol/L; 3 – 0.25 mol/L.

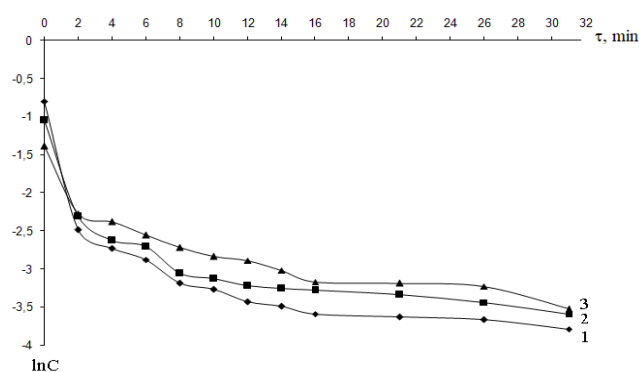


Fig. 6. Dependence of the natural logarithm of ferrous sulphate concentration on the process time $t = 100\text{ }^\circ\text{C}$; $n = 8$; initial concentration of ferrous sulphate: 1 – 0.45 mol/L; 2 – 0.35 mol/L; 3 – 0.25 mol/L.

Since the reaction of ferrous sulfate with ammonium carbonate can be divided into two stages:

- 1) the formation of $\text{Fe}(\text{OH})_2$ – 0–14 min of the process;

- 2) the formation of Fe_3O_4 – 14–16 min, it can be constructed the graphs corresponding to the reaction for obtaining these products (Figs. 7 and 8).

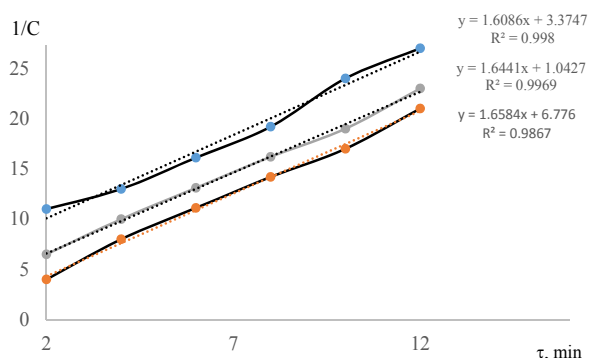


Fig. 7. Dependence of the inverse concentration of ferrous sulfate on the process time $t = 100\text{ }^\circ\text{C}$; $n = 8$; $\tau = 2\text{--}14$ min; initial ferrous sulphate concentration; 1 – 0.45 mol/L; 2 – 0.35 mol/L; 3 – 0.25 mol/L

The obtained dependences indicate that the reaction between iron sulphate and ammonium carbonate is a second-order reaction and can be described by the equation:

$$-\frac{dC}{d\tau} = kC^2$$

where k – the reaction rate constant, L/min mol; τ – the reaction time, min; C – the concentration of the reactant, mol/L.

From the Figs. 7–8, we can determine the rate constants. They constitute, for 0–14 min – 1.645 L/min mol; $\tau = 16$ –31 min – 0.654 L/min mol.

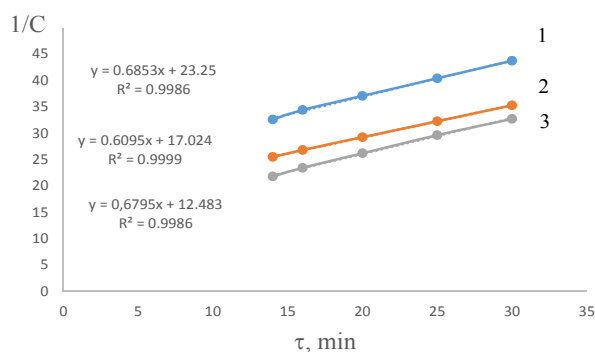


Fig. 8. Dependence of the inverse concentration of ferrous sulfate on the process time $t = 100$ °C; $n = 8$; $\tau = 16$ –31 min, initial ferrous sulphate concentration: 1 – 0.45 mol/L; 2 – 0.35 mol/L; 3 – 0.25 mol/L

4. Conclusions

Magnetite, formed in a solution of ferrous sulphate during the hydrolysis of ammonium carbonate, has a homogeneous phase composition and a cubic crystal structure. The reaction of magnetite formation in the range of concentrations and temperatures under study passes in two stages – the formation of ferrous hydroxide and its oxidation to magnetite. Both reactions are described by a formal kinetic equation of the second order. The rate constant of the first stage is 2.5 times faster than the rate constant of the second reaction. The formation of magnetite occurs in the second stage. The obtained parameters of the process can be used to substantiate the technology of magnetite synthesis using an optimized phase composition.

References

- [1]. M.J. Ryan, A.D. Kney, T.L. Carley, *Appl. Geochem.* 79 (2017) 27–35. DOI: 10.1016/j.apgeochem.2017.01.019
- [2]. F.Q. Mariani, K.W. Borth, M. Müller, M. Dalpasquale, F.J. Anaissi, *Dyes Pigments* 137 (2017) 403–409. DOI: 10.1016/j.dyepig.2016.10.024
- [3]. T.Q. Bui, S.N.-C. Ton, A.T. Duong, H.T. Tran, *J. Sci. Adv. Mater. Devices* 3 (2018) 107–112. DOI: 10.1016/j.jsamd.2017.11.002
- [4]. H. Shirinova, L.Di Palma, F. Sarasini, J. Tirillò, M.A. Ramazanov, F. Hajiyeva, D. Sannino, M. Polichetti, A. Galluzzi, *Chem. Eng. Trans.* 47 (2016) 103–108. DOI: 10.3303/CET1647018
- [5]. W. Jiang, K.L. Lai, H. Hu, X.B. Zeng, F. Lan, K.X. Liu, Y. Wu, Z.W. Gu, *J. Nanopart. Res.* 13 (2011) 5135–5145. DOI: 10.1007/s11051-011-0495-8
- [6]. W. Wang, B. Tang, B. Ju, S. Zhang, *RSC Adv.* 5 (2015) 75292–75299. DOI: 10.1039/C5RA14354C
- [7]. U.S. Khan, A. Rahim, N. Khan, N. Muhammad, F. Rehman, K. Ahmad, J. Iqbal, *Mater. Chem. Phys.* 189 (2017) 86–89. DOI: 10.1016/j.matchemphys.2016.12.047
- [8]. X. Liang, H. Xu, J. Chen, J. Sun, Y. Yang, *Glass Physics and Chemistry.* 37 (2011) 330–342. DOI: 10.1134/S1087659611030084
- [9]. M.S. Sadjadi, A. Sharafi, N. Farhadyar, *J. Nano Res-SW* 21 (2013) 37–42. DOI: 10.4028/www.scientific.net/JNanoR.21.37
- [10]. S. Franger, P. Berthet, J. Berthon, *J. Solid State Electr.* 8 (2004) 218–223. DOI: 10.1007/s10008-003-0469-6
- [11]. N. Mizutani, T. Iwasaki, S. Watano, T. Yanagida, H. Tanaka, T. Kawai, *B. Mater. Sci.* 31 (2008) 713–717. DOI: 10.1007/s12034-008-0112-3
- [12]. W. Wu, X. Xiao, S. Zhang, H. Li, X. Zhou, C. Jiang, *Nanoscale Res. Lett.* 4 (2009) 926–931. DOI: 10.1007/s11671-009-9342-6
- [13]. J. Boháček, J. Šubrt, T. Hanslík, J. Tláškal, *J. Mater. Sci.* 28 (1993) 2827–2832. DOI: 10.1007/BF00356226
- [14]. A. Šolcová, J. Šubrt, J. Vinš, F. Hanousek, V. Zapletal, J. Tláškal, *Collect. Czech. Chem. Commun.* 46 (1981) 3049–3056. DOI: 10.1135/cccc19813049
- [15]. S.Z. Kalaeva, V.M. Makarov, N.S. Yamanina, I.N. Zakharova, A.N. Solovyova, M.S. Maltseva, A.M. Shipilin, M.E. Terzi, *Izvestiya Vysshikh Uchebnykh Zavedeniy Seriya "Khimiya I Khimicheskaya Tekhnologiya"* [Russian Journal of Chemistry and Chemical Technology] 58 (2015) 51–54 (in Russian).
- [16]. L.A. Bondar', N.V. Abramov, V.N. Mishchenko, P.P. Gorbik, *Colloid J.* 72 (2010) 1–5. DOI: 10.1134/S1061933X10010011
- [17]. V.S. Pokatilov, A.S. Sigov, A.O. Konovalova, *Bull. Russ. Acad. Sci.: Phys.* 76 (2012) 737–739. DOI: 10.3103/S1062873812070283
- [18]. E.V. Shinkareva, T.G. Lazareva, O.A. Shchurevich, L.A. Kurakevich, *Russ. J. Appl. Chem.* 78 (2005) 1596–1599. DOI: 10.1007/s11167-005-0568-5

- [19]. L. Hu, A. Percheron, D. Chaumont, C.-H. Brachais, *J. Sol-Gel Sci. Techn.* 60 (2011) 198. DOI: 10.1007/s10971-011-2579-4
- [20]. V. Akinwekomi, J.P. Maree, C. Zvinowanda, V. Masindi, *Journal of Environmental Chemical Engineering* 5 (2017) 2699–2707. DOI: 10.1016/j.jece.2017.05.025
- [21]. Y.U. Wang, Y. Peng, Y. Zheng, *Trans. Nonferrous Met. Soc. China* 27 (20017) 211–219. DOI: 10.1016/S1003-6326(17)60024-4
- [22]. L.A. Frolova, *Metallurgical and Mining Industry* 4 (2014) 65–69.
- [23]. L. Frolova, A. Pivovarov, T. Butyrina, *Pigm. Resin Technol.* 46 (2017) 356–361. DOI: 10.1108/PRT-07-2016-0073
- [24]. L. Frolova, A. Derimova, I. Galivets, M. Savchenko, A. Khlopytskyi, *Eastern-European Journal of Enterprise Technologies* 6 (2016) 64–68. DOI: 10.15587/1729-4061.2016.85123
- [25]. V.N. Alekseev, *Kolichestvennyiy analiz. AlyanS*, 2007, p. 504 (in Russian).